

# Determination of Macromolecular Concentration Following Direct Infusion into Hydrogel using Contrast-Enhanced MRI

Xiaoming Chen, Garrett W. Astary, Thomas H. Mareci, and Malisa Sarntinoranont

**Abstract**— Direct tissue infusion has emerged as a promising drug delivery method for treating diseases of the nervous system because the blood-brain or blood-spinal cord barriers are circumvented. Determination of the spatial distribution of therapeutic agents after infusion is important in evaluating the efficacy of treatment and optimizing infusion protocols. In this study, we provide a methodology to determine the concentration distribution of Gd-labeled tracers using contrast-enhanced MRI. An 11.1 T magnet system was used to image infusion of Gd-DTPA labeled albumin (Gd-albumin) into an agarose-based hydrogel. By using data from preliminary scans, Gd-albumin distribution was determined from the signal intensity of the MR images. As an initial validation test, these concentration profiles were compared with distribution profiles predicted for porous media transport by convection and diffusion. Comparison of model results show good correlation between predicted distributions. In future studies, the presented methodology may be used to estimate the distribution of Gd-tracer following infusion directly into tissue.

**Keywords**— Agarose gel, Albumin, Convection enhanced delivery, Contrast agent, CED, Gd-DTPA, MRI

## I. INTRODUCTION

The blood-brain and blood-spinal cord barriers act as major impediments in systemic delivery of macromolecular therapeutic agents to the brain and spinal cord. Direct infusion of therapeutic agents into the parenchyma of nervous tissue circumvents these vascular barriers and enhances the interstitial (extracellular) transport by convective flow which distributes compounds over a larger region than diffusion alone. Recently, direct tissue infusion, e.g., convection-enhanced delivery (CED), has emerged as a promising drug delivery method for treating diseases of the nervous system. Previous nervous tissue infusion studies have shown CED to be reproducible and clinically safe [1-3].

Concentration distribution of therapeutic agents after infusion is significantly related to the CED protocol, e.g., selection of infusion site, infusate concentration, and

infusion rate, and is critical to the efficacy of treatment. Computational models of direct infusion have been developed to predict distribution profiles of macromolecular agents in tissue interstitium [4-6]. Experimental methods have also been investigated to monitor the concentration distribution during CED [1, 3]. In these studies, contrast-enhanced MR imaging of infused macromolecular agents has been completed to determine their distribution. These studies generally assume signal intensity is proportional to agent concentration in tissue. Relating MRI signal intensity to concentration by comparison with calibration samples has also been conducted [7]. Such a method may be difficult for *in vivo* measurement since calibration samples of living tissue may not be available. To improve monitoring of the evolving concentration distribution during CED, additional imaging studies to relate signal intensity to concentration profiles are required. Previous studies [8-11] show that absolute Gd-DTPA concentration can be quantified using MRI. Hittmair *et al.* [9] used the relative change of MR signal before and after adding contrast agent to calculate the concentration. Morkenborg *et al.* [12] used different pulse sequences to quantify the Gd-DTPA concentration in human plasma. Contrast-enhanced MRI offers a promising method to quantify concentration. However, standardization of data acquisition and analysis of this technique is still lacking [10].

The purpose of this study is to provide a methodology to quantify infusion concentration distributions using contrast-enhanced MRI. An 11.1 T magnet system was used to obtain preliminary scans and image the infusion of Gd-DTPA labeled albumin (Gd-albumin) into an agarose gel phantom. The relationship between signal intensity of MR images and agent concentration is presented. Selection of experimental parameters is also discussed. As an initial validation test, these concentration profiles were compared with distribution profiles predicted for porous media transport by convection and diffusion. In future studies, this developed methodology may be used to determine distribution of infused Gd-tracer directly into tissues.

## II. METHODS

### A. Theoretical Analysis

**Contrast-enhanced MRI analysis.** Signal intensity from conventional  $T_1$ -weighted spin-echo MR imaging is expressed as [13]

Manuscript received April 2, 2007. This work was supported in part by the National Institutes of Health under Grant 1R21NS052670-01A1.

M. Sarntinoranont is with the Department of Mechanical & Aerospace Engineering, University of Florida, Gainesville, FL 32611. (phone: 352-392-8404; fax: 352-392-7303; e-mail: msarnt@ufl.edu).

X. Chen is with the Department of Mechanical & Aerospace Engineering (e-mail: xmchen@ufl.edu).

G.W. Astary is with the Department of Biomedical Engineering (e-mail: gwastary@ufl.edu).

T.H. Mareci is with the Department of Biochemistry and Molecular Biology (e-mail: thmareci@ufl.edu).

$$S = S_0(1 - e^{-TR/T_1})e^{-TE/T_2} \quad (1)$$

where  $TR$  is the time for recovery;  $TE$  is the time of echo;  $S_0$  is the maximum signal intensity determined by proton density, relaxation times, and instrument factors, such as the resonance frequency, and the receiving coil geometry. The effects of contrast agent on relaxation rate are given by [10]

$$\frac{1}{T_1} = \frac{1}{T_{10}} + R_1 \cdot c \quad \frac{1}{T_2} = \frac{1}{T_{20}} + R_2 \cdot c \quad (2)$$

where  $T_{10}$  and  $T_{20}$  are the relaxation times without contrast agent;  $T_1$  and  $T_2$  are the relaxation times with contrast agent at a concentration  $c$ ;  $R_1$  and  $R_2$  are the longitudinal and transverse relaxivities of the contrast agent, respectively. Substituting Eq. 2 into Eq. 1 results in the relation

$$S(c) = S_0[1 - e^{-TR(1/T_{10} + R_1 \cdot c)}] \cdot e^{-TE(1/T_{20} + R_2 \cdot c)} \quad (3)$$

which is the enhanced signal intensity with a contrast agent. The signal enhancement is then defined as

$$\frac{S(c)}{S(0)} = \frac{[1 - e^{-TR(1/T_{10} + R_1 \cdot c)}] \cdot e^{-TE(1/T_{20} + R_2 \cdot c)}}{[1 - e^{-TR/T_{10}}] \cdot e^{-TE/T_{20}}} \quad (4)$$

where  $S(c)$  is the signal intensity for concentration,  $c$ ;  $S(0)$  is the signal intensity for zero concentration. For  $T_1$ -weighted imaging, the infusion concentration was selected so that  $e^{-TE \cdot R_2 \cdot c} \approx 1$ . Thus for small  $TE$  value,

$$c = \frac{1}{R_1} \left[ \frac{1}{TR} \ln \frac{S(0)}{S(0) - S(c) \cdot (1 - e^{-TR/T_{10}})} - \frac{1}{T_{10}} \right] \quad (5)$$

Equation 5 relates the signal intensity to the contrast agent concentration for known values of  $R_1$ ,  $S(0)$ , and  $T_{10}$ .

**Noise removal.** A low SNR (signal-to-noise ratio) may significantly affect the accuracy of estimated concentrations. Zero-mean Gaussian noise was assumed and the confounding effect of noise on the measured signal was removed by using [14]

$$\langle S \rangle = \sqrt{\langle M^2 \rangle - 2\sigma^2} \quad (6)$$

where  $\langle S \rangle$  is the average signal intensity within a region of interest (ROI);  $\langle M^2 \rangle$  is the average of the square measured-signal-intensity; and  $\sigma^2$  is the variance of observed noise.

**Porous media model of direct infusion.** Infusion into the hydrogel can be modeled as an infusion into a rigid porous media. Fluid flow in rigid porous media is described by Darcy's law

$$\phi \mathbf{v}^f = -k \nabla p \quad (7)$$

where  $\phi$  is the porosity (i.e. fractional volume of fluid in the porous media);  $k$  is the hydraulic permeability;  $\mathbf{v}^f$  is the fluid velocity in the porous media; and  $p$  is the fluid pressure.

Transport of a non-binding, macromolecular agent such as

albumin is described by the convection-diffusion equation

$$\frac{\partial c}{\partial t} + \nabla \cdot (c \mathbf{v}^f - \mathbf{D}_{\text{eff}} \cdot \nabla c) = 0 \quad (8)$$

where  $c$  is the concentration in hydrogel, and  $\mathbf{D}_{\text{eff}}$  is the effective diffusivity of Gd-albumin in the hydrogel. We modeled infusion into a spherical porous media (7.5 mm radius) with a spherical infusion cavity (75  $\mu\text{m}$  radius) at the center. Constant concentration and constant flow rate (0.29  $\mu\text{L}/\text{min}$ ) were applied to the embedded infusion cavity. Zero pore pressure was applied to the outer boundary surfaces.

A finite element model for infusion into the porous media was implemented using COMSOL (v. 3.0, COMSOL, Inc., Burlington, MA). Fluid velocity,  $\mathbf{v}^f$ , was solved first using Darcy's law ( $k = 1.427 \times 10^{-12} \text{ m}^4 \text{ N}^{-1} \text{ s}^{-1}$ , measured using a permeameter system in our lab). By using the obtained fluid field, convection-diffusion transport of Gd-albumin was solved using different diffusivities,  $D_{\text{eff}} = 1.0, 5.0, \text{ and } 7.12 (10^{-11} \text{ m}^2/\text{s})$ . The latter two values were experimentally measured at temperatures of 25 and 37°C, respectively, for bovine serum albumin diffusion in 1% (w/w) agarose gel [15]. Since the signal intensity of a pixel in the MR image is an average over a voxel (0.229 mm  $\times$  0.229 mm  $\times$  1.0 mm), concentration obtained from the simulation was adjusted accordingly by averaging the concentration along a 1.0 mm line (thickness of slice) in slice direction. Porosity of the gel was estimated by  $Vi/Vd$ , which was  $\sim 0.6$ .  $Vd$  is the distribution volume and  $Vi$  is the volume infused.

## B. Materials and Procedures

**Materials.** 25 mg/mL Gd-albumin (Galbumin, BioPAL Inc., Worcester, MA) was diluted with deionized water into  $\sim 100 \mu\text{L}$  calibration vials at concentrations of 2, 4, 6, 8, 10, 11, 12, 13, 14, 15 mg/mL. Calibration vials based on this series were used to obtain  $R_1$  and  $R_2$  values. A diluted concentration of 10 mg/mL was used for hydrogel infusion studies (see Imaging Procedure).

For infusion studies,  $\sim 15 \text{ mL}$  of 1% (w/w) agarose-based hydrogel (TreviGel 5000, Trevigen, Inc., Gaithersburg, MD) was prepared in 15 mL plastic test tubes. A silica cannula (ID=50  $\mu\text{m}$ , OD=147  $\mu\text{m}$ ) was inserted  $\sim 2 \text{ cm}$  into the gel. This cannula was coupled to a non-metallic hydraulic drive which consisted of a modified gas-tight syringe (Hamilton, Reno, NV) and PEEK tubing. The hydraulic drive allowed for remote placement of the syringe pump which drove infusion at a constant infusion rate of 0.29  $\mu\text{L}/\text{min}$  over 91 min (total infusion volume of 26  $\mu\text{L}$ ).

**Imaging Procedure.**  $T_1$  and  $T_2$  values of calibration vials, with various concentrations of the contrast agent, were measured using a Bruker Avance 11.1 T horizontal bore magnet system (Bruker NMR Instruments, Billerica, MA). A custom quadrature birdcage MR coil was used for excitation and detection. For  $T_1$  measurements, a spin echo (SE) sequence with  $TR = 250, 500, 1000, 2000, 4000 \text{ ms}$ , and  $TE = 15 \text{ ms}$  was used with 2 averages. For  $T_2$  measurement, a

SE sequence with minimized diffusion weighting, and with  $TE = 15, 30, 45, 60, 75, 100, 125$  ms, and  $TR = 2000$  ms was used with 3 averages. During infusion, MR imaging was performed with  $TR = 330$  ms,  $TE = 9.4$  ms ( $T_1$ -weighted) with 6 averages. For all sequences, the image resolution was  $0.229 \text{ mm} \times 0.229 \text{ mm} \times 1.0 \text{ mm}$  per voxel. All imaging procedures were conducted at room temperature ( $\sim 25 \text{ }^\circ\text{C}$ ).

Using the measured values,  $R_1$  and  $R_2$  values were calculated using Eq. 2.  $T_{10}$  and  $T_{20}$  of the gel and  $R_1$  and  $R_2$  values were then used to estimate a range of infusion concentrations,  $c_{in}$ , which provides distinct signal contrast at different concentrations of contrast agent. From this result,  $c_{in} = 10 \text{ mg/mL}$  (0.143 mmol/L) was selected as an appropriate concentration for infusion. Following pre-infusion MR scans to measure  $S(0)$ , infusion and simultaneous MR scanning were performed.

### III. RESULTS

#### A. Measurement of $T_{10}$ , $T_{20}$ , $R_1$ , and $R_2$ for the hydrogel

Table 1 shows the measured parameter values using  $T_1$  and  $T_2$  measurement. It is found that the measured  $T_1$  and  $T_2$  values are close to those of water [13]. This is reasonable given that the hydrogel is composed of 99% (w/w) water. Also,  $R_1$  and  $R_2$  values of the 1% agarose-based gel was assumed to be equivalent to those measured in water because of the high water content in the gel [11, 16].

TABLE 1. PARAMETER VALUES FOR 1% (W/W) AGAROSE GEL.

$T_{10}$ (sec)	$T_{20}$ (sec)	$R_1$ (L/mmol-s)*	$R_2$ (L/mmol-s)*
$3.518 \pm 0.323$	$0.117 \pm 0.001$	$22.27 \pm 0.56$	$42.27 \pm 2.53$

\* approximated by the values measured in water.

#### B. Infusion concentration analysis

For  $T_1$ -weighted imaging, signal intensity increased with the concentration for a low concentration range and decreased at concentrations higher than a threshold value (Fig. 1). This threshold changes for different  $TR$  values.

To map the signal intensity with agent concentrations, a range of low concentrations is desired due to a nearly linear signal versus concentration relationship. Also, a larger  $dS/dc$  value is desired since it gives a larger contrast range, i.e., a broader range of signal intensity for a given range of concentration. A longer  $TR$  value gives a larger contrast range but increases the imaging time. For this study,  $TR = 330$  ms was found to be an appropriate choice (Fig. 1).

#### C. MRI results

Figure 2 shows a MR image after infusion of Gd-Albumin for 91 min. The signal profile along the radial direction was obtained by sampling in the small square ROIs which were aligned in the radial direction. The location of the silica cannula infusion site was identified as a black dot in the image center.

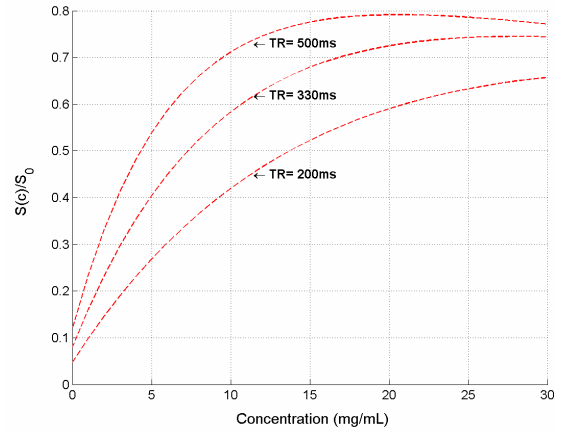


Figure 1. Theoretical concentration versus signal intensity relationship (Eq. 3;  $T_1$ -weighted imaging). Parameter values are based on Table 1.

Figure 3 compares concentration profiles obtained by simulation and MRI experiments. The MR-derived concentration was obtained by converting the signal intensity to Gd-albumin concentration using Eq. 5. A maximum MR-derived concentration of 6.4 mg/mL was determined near the infusion site. This value is consistent with the estimated porosity,  $\sim 0.6$ , and the infusate concentration of 10 mg/mL. MR-derived concentration data corresponds well with the porous media transport simulation profiles at higher diffusivity, e.g.,  $D_{eff} = 7.12 \times 10^{-11} \text{ m}^2/\text{s}$  ( $R^2 = 0.91$ ). A good match was found in the high concentration regions. However, MR-derived concentrations were slightly higher than those predicted by the porous media model at low concentrations.

### IV. DISCUSSION

In this study, we presented a methodology to quantify the distribution of Gd-albumin following direct infusion into a hydrogel. We used  $T_1$ -weighted spin-echo imaging to obtain the spatial-temporal signal evolution with infusion. Signal intensity was converted to Gd-albumin concentration using Eq. 5, with the measured  $R_1$ ,  $S(0)$ , and  $T_{10}$  values. The MR-derived concentration profile showed a good match with porous media simulation results. In addition, infusion concentration analysis showed that infusate concentration and experimental imaging parameters, e.g.  $TR$  and  $TE$ , should be carefully chosen to obtain a broad contrast range of signal intensity and a unique signal-concentration mapping for a given range of concentration.

The signal-concentration relation (Eq. 5) was based on  $T_1$ -weighted imaging, and it assumed that  $e^{-TE \cdot R_2 \cdot c} \approx 1$ . This assumption is reasonable since using the parameters in this study,  $e^{-TE \cdot R_2 \cdot c} = 0.97 \sim 0.99$ . This signal-concentration relationship was also not sensitive to changes of the  $R_2$  value for the range of parameters in this study. The signal-concentration relationship may also be obtained by using Eq. 3, which has an unknown  $S_0$ .  $S_0$  may be obtained during  $T_1$  or  $T_2$  measurement. Hittmair *et al.* [9] determined

concentrations by calculating an enhancement factor, which is a function of  $S_0$ . To obtain  $S_0$ , very low flip angle sequence was used. However,  $S_0$  is environment-dependent, e.g. depending on the receiving coil, and may be different for each MR measurement. In addition, SE sequence was used and each scan took  $\sim 3$ min in this study. This time resolution is acceptable given the slow radial velocities of albumin transport in the gel (average of 0.022 mm/min during the 91 min infusion with a maximum of  $\sim 0.060$  mm/min at the beginning of infusion).

In this study, we used an agarose-based hydrogel phantom as our infusion media and found good agreement between theory and experiment. Quantitative measure of interstitial drug distributions is important in determining efficacy of treatment and optimizing infusion protocols. In future studies, the presented methodology may be applied to direct infusion into biological tissue.

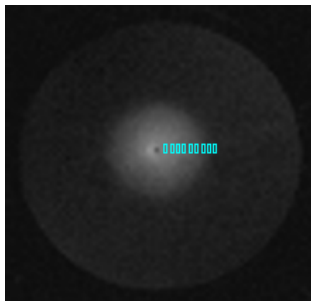


Figure 2. A MR image after infusion of Gd-Albumin for 91min. The infusion cannula/site was indicated by a black dot in the image center. The signal profile in the radial direction was obtained by sampling in small ROIs ( $\sim 20$  pixels in each square).

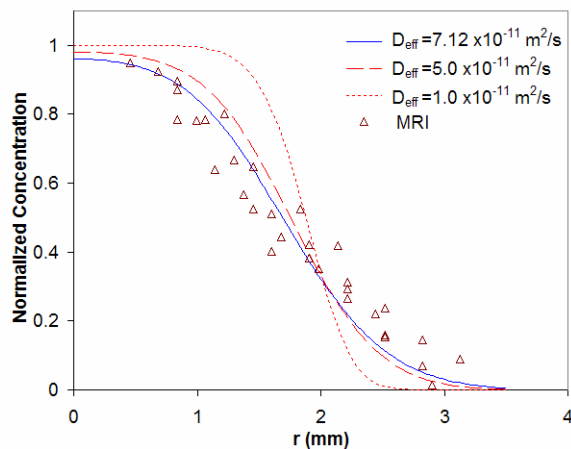


Figure 3. MR-derived concentration compared with predicted porous media transport profiles at time = 91 min. Concentration was normalized by dividing by the maximum MR-derived concentration, 6.4 mg/mL.  $D_{eff}$  was experimentally measured at different temperatures by Liang *et al.* [15].  $R^2 = 0.91, 0.84,$  and  $0.40$  for  $D_{eff} = 7.12, 5.0,$  and  $1.0$  ( $10^{-11}$  m<sup>2</sup>/s), respectively.

## V. ACKNOWLEDGEMENTS

We would like to thank Hector Sepulveda, Jessica Meloy, Zachary Bryan, and Sung Jin Lee for technical assistance with experiments.

## REFERENCES

- [1] R. H. Bobo, D. W. Laske, A. Akbasak, P. F. Morrison, R. L. Dedrick, and E. H. Oldfield, "Convection-enhanced delivery of macromolecules in the brain," *Proc. Natl. Acad. Sci.*, vol. 91, pp. 2076-2080, 1994.
- [2] J. D. Wood, R. R. Lonser, N. Gogate, P. F. Morrison, and E. H. Oldfield, "Convective delivery of macromolecules into the naive and traumatized spinal cords of rats," *J. Neurosurg.*, vol. 90, pp. 115-120, 1999.
- [3] R. R. Lonser, S. Walbridge, J. A. Butman, H. A. Walters, K. Garmestani, A. O. Vortmeyer, M. W. Brechbiel, and E. H. Oldfield, "Successful safe perfusion of the primate brainstem with a macromolecule: In vivo magnetic resonance imaging of macromolecular distribution during infusion," *Neurosurg.*, vol. 51, pp. 551-551, 2002.
- [4] Z.-J. Chen, W. C. Broaddus, R. R. Viswanathan, R. Raghavan, and G. T. Gillies, "Intraparenchymal drug delivery via positive-pressure infusion: experimental and modeling studies of poroelasticity in brain phantom gels," *IEEE Trans. Biomed. Eng.*, vol. 49, pp. 85-96, 2002.
- [5] P. J. Basser, "Interstitial pressure, volume, and flow during infusion into brain tissue," *Microvasc. Res.*, vol. 44, pp. 143-165, 1992.
- [6] M. Sarntinoranont, R. K. Banerjee, R. R. Lonser, and P. F. Morrison, "A computational model of direct interstitial infusion of macromolecules into the spinal cord," *Ann. Biomed. Eng.*, vol. 31, pp. 448-461, 2003.
- [7] H. Kim, M. J. Lizak, G. Tansey, K. G. Csaky, M. R. Robinson, P. Yuan, N. S. Wang, and R. J. Lutz, "Study of ocular transport of drugs released from an intravitreal implant using magnetic resonance imaging," *Ann. Biomed. Eng.*, vol. 33, pp. 150-164, 2005.
- [8] M. F. Tweedle, P. Wedeking, J. Telsler, C. H. Sotak, C. A. Chang, K. Kumar, X. Wan, and S. M. Eaton, "Dependence of MR Signal Intensity on Gd Tissue Concentration over a Broad Dose Range," *Magn. Reson. Med.*, vol. 22, pp. 191-194, 1991.
- [9] K. Hittmair, G. Gomiscek, K. Langenberger, M. Recht, H. Imhof, and J. Kramer, "Method For the Quantitative Assessment of Contrast Agent Uptake in Dynamic Contrast-Enhanced MRI," *Magn. Reson. Med.*, vol. 31, pp. 567-571, 1994.
- [10] T. P. L. Roberts, "Physiologic measurements by contrast-enhanced MR imaging: Expectations and limitations," *J. Magn. Reson. Imaging*, vol. 7, pp. 82-90, 1997.
- [11] G. J. Stanisz and R. M. Henkelman, "Gd-DTPA relaxivity depends on macromolecular content," *Magn. Reson. Med.*, vol. 44, pp. 665-667, 2000.
- [12] J. Morkenborg, M. Pedersen, F. T. Jensen, H. Stodkilde-Jorgensen, J. C. Djurhuus, and J. Frokiaer, "Quantitative assessment of Gd-DTPA contrast agent from signal enhancement: an in-vitro study," *Magn. Reson. Imaging*, vol. 21, pp. 637-643, 2003.
- [13] E. M. Haacke, R. W. Brown, M. R. Thompson, and R. Venkatesan, *Magnetic Resonance Imaging: Physical Principles and Sequence Design*. New York: John Wiley & Sons, Inc, 1999.
- [14] C. G. Koay and P. J. Basser, "Analytically exact correction scheme for signal extraction from noisy magnitude MR signals," *J. Magn. Reson.*, vol. 179, pp. 317-322, 2006.
- [15] S. M. Liang, J. Xu, L. H. Weng, H. J. Dai, X. L. Zhang, and L. N. Zhang, "Protein diffusion in agarose hydrogel in situ measured by improved refractive index method," *J. Controlled Release*, vol. 115, pp. 189-196, 2006.
- [16] K. M. Donahue, D. Burstein, W. J. Manning, and M. L. Gray, "Studies of Gd-Dtpa Relaxivity and Proton-Exchange Rates in Tissue," *Magn. Reson. Med.*, vol. 32, pp. 66-76, 1994.